Cement and Concrete Research 88 (2016) 211–216

Contents lists available at ScienceDirect

Cement and Concrete Research

journal homepage: www.elsevier.com/locate/cemconres

Electrochemical behaviour of steel in mortar and in simulated pore solutions: Analogies and differences

Gustavo S. Duffó, Silvia B. Farina *

[a] Comisión Nacional de Energía Atómica – Gerencia Materiales, Departamento Corrosión, Av. Gral. Paz 1499 – (1650) San Martín, Buenos Aires, Argentina
[b] Universidad Nacional de Gral. San Martín, Av. Gral. Paz 1499 – (1650) San Martín, Buenos Aires, Argentina
[c] Consejo Nacional de Investigaciones Científicas y Técnicas, Av. Gral. Paz 1499 – (1650) San Martín, Buenos Aires, Argentina

ARTICLE INFO

Article history:
Received 13 February 2015
Accepted 6 July 2016
Available online xxxx

Keywords:
C. Corrosion
C. Electrochemical properties
D. Reinforcement
Chloride
E. Mortar

ABSTRACT

On evaluating the corrosion resistance of concrete, it is frequent to perform electrochemical tests in the so called *simulated pore solutions* (SPS) to replace tests performed in concrete specimens. Besides, to study the effect of the chloride content in concrete, chloride ions are added to the SPS. However, it is not obvious whether the SPS simulate the electrochemical behaviour of steel in concrete. Another concern is related to the relationship between the chloride content in concrete and the chloride content of a SPS. To investigate this issue a comparison between the polarization curves of steel in mortar and in SPS was performed. It was found that the SPS is not fully representative of the corrosion behaviour of steel in mortar but it yields conservative results. The relationship between the chloride content in mortar and in SPS that yields similar behaviour is not straightforward but depends on the electrochemical parameter considered.

1. Introduction

For several practical reasons the corrosion of steel bars used as reinforcement in concrete is frequently performed using the so called *simulated pore solutions* to replace tests performed in reinforced concrete specimens. These solutions contain alkalis and are basically developed aiming at simulate the pH of the real pore solution (between 12.5 and 13.5). Different formulations are found in the literature [1–9], but they differ slightly in composition, being $Ca(OH)_2$, KOH and NaOH the main constituents. Besides, to study the effect of the chloride content in concrete, chloride ions are usually added to the simulated pore solutions.

Numerous works are published regarding the behaviour of different types of rebars (carbon steel, galvanized steel, stainless steel, etc.) in simulated pore solutions [8,10–12 just to mention a few of them]. Some authors studied the threshold chloride level for localized corrosion [5,8,9,13], others studied the effect of pitting corrosion inhibitors [14–17], while others evaluated the role of the microstructure and/or surface state on the corrosion behaviour [18–21]. The electrochemical techniques used are the common ones, such as electrochemical impedance spectroscopy, polarization curves, measurements of linear polarization resistance, etc. The objective of these works is to predict the behaviour of the materials in real service. However, the following question arises: do the simulated pore solutions simulate the electrochemical behaviour shown by the steel embedded in cementitious materials (mortar or concrete)? And, what is the relationship between the chloride content in concrete/mortar and the chloride content of a simulated pore solution? To answer these questions it is essential to compare the electrochemical behaviour observed in simulated pore solutions with that obtained in concrete/mortar specimens. Though this seems to be obvious, such a study is not found in literature. Up to the authors knowledge, the only work that mentions this issue is due to Kouřil et al. [8], who state that "the concentrations of 15 and 80 g Cl^-/l were found to be close to 0.4 and 3 wt.% Cl^-/cem, respectively, when concrete moisture is in equilibrium with RH (*relative humidity*) 90% air". However, Kouřil et al. did not mention either the origin of this relationship or the experimental tests that support it.

The objective of this paper is, in general terms, to determine up to what extent the use of simulated pore solutions allows predicting the behaviour of rebars embedded in concrete/mortar. A comparison between the polarization curves of steel bars embedded in mortar with and without chloride content and with different aging times at 98% RH, and those obtained for steel bars immersed in a frequently used simulated pore solution [3] with different chloride ion additions, were

* Corresponding author at: Comisión Nacional de Energía Atómica – Gerencia Materiales, Departamento Corrosión, Av. Gral. Paz 1499 – (1650) San Martín, Buenos Aires, Argentina.
E-mail address: farina@cnea.gov.ar (S.B. Farina).

http://dx.doi.org/10.1016/j.cemconres.2016.07.007
0008-8846/

performed. The comparison was performed using different electrochemical parameters, such as the corrosion potential, the passive current density, the pitting potential and the polarization resistance.

2. Materials and methods

Experiments were performed on mortar prismatic specimens measuring 7 × 7 × 6 cm^3, as shown in Fig. 1. Four 6 mm diameter and 60 mm length carbon steel smooth rods, symmetrically embedded in the prisms, were used as working electrodes (WE). The rods were used in the *as-received* condition, and they were degreased with ethyl acetate. These rods were embedded in mortar and the mortar-air interface was isolated with adhesive tape in order to avoid crevice corrosion due to differential aeration. The embedded ends of the rods were also covered with adhesive tape, to obtain an active surface area of 5.7 cm^2. The chemical composition of the rods was (in wt.%): C, 0.39; Si, 0.30; Mn, 0.66; P, 0.007; S, 0.005; Cr, 0.04; Ni, 0.02; Mo, <0.003, Fe, balance.

Mortar specimens were prepared with a cement/sand/water ratio of 1/3/0.6 with chloride additions (as NaCl) of 0, 0.5, 2, 5 and 10%, relative to cement weight. The cement used was Sulphate Resistant Portland Cement (CPN 40 ARS, Loma Negra™) and its chemical composition is shown in Table 1. The sand used was a standard one (CEN-NORMSAND DIN EN 196-1).

Three specimens for each condition were prepared (so that for each chloride content, 12 steel rods were available for electrochemical tests). The mortar was cast in metallic moulds and after curing for 24 h, the mortar blocks were taken from the moulds and kept at 98% RH at room temperature for 28 days (*moist curing*). The compressive strength of the mortar specimens after 28 days was 22.6 ± 2.3 MPa. The three specimens prepared for each chloride content were kept at 98% RH for periods of 0, 90 and 180 days after the moist curing. After these aging times, the electrochemical tests were performed.

A three electrode configuration was used to perform the electrochemical tests (Fig. 1). A stainless steel cylinder of 7 cm diameter with a central hole to place a saturated calomel electrode (SCE) as reference electrode (RE) was used as counter electrode (CE). A damp cloth was used to allow electrical conductivity between the electrodes.

Cyclic potentiodynamic polarization curves were drawn at a scan rate of 0.2 mV/s using a Gamry Ref. 600 potentiostat. Before starting the measurements, the open circuit potential was measured for 1 h and, in all cases, after this period, the open circuit potential reached a stationary value. The scan started at a potential 300 mV lower than the open circuit potential, and the reverse scan started when the circulating current density reached 0.2 mA/cm^2. The resistance of the mortar to the electrical current was obtained as the real impedance measured when applying a sinusoidal signal ($\Delta V = 10$ mV, $\nu = 1$ kHz) in the three electrode configuration. The results were used for the Ohmic drop correction.

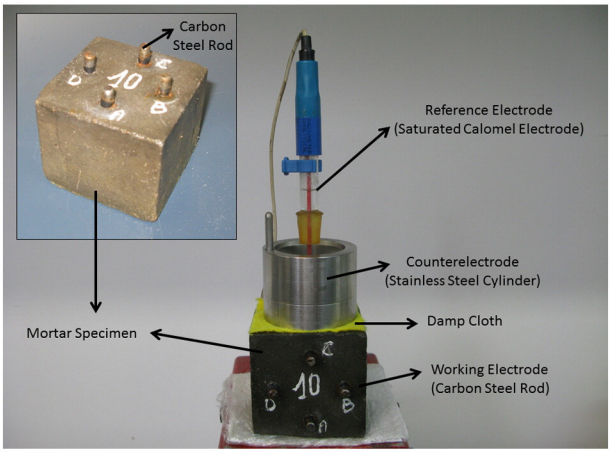

Fig. 1. Prismatic mortar specimens and cell configuration for electrochemical tests.

Table 1
Chemical composition of the cement used in the present work.

Compound	wt.%
SiO_2	21.4
CaO	64.5
Al_2O_3	3.46
Fe_2O_3	4.90
SO_3	2.04
MgO	0.82
Na_2O	0.07
K_2O	0.93
Cl^-	<0.01
S^{2-}	<0.01

For the tests in aqueous solutions, the measurements were performed in an acrylic cell with a platinum CE. Potentials were measured through a Luggin capillary with a SCE acting as reference electrode. The simulated pore solution (SPS) used was one frequently found in literature [3], whose composition is: 7.4 g of NaOH and 35.6 g of KOH per litre of $Ca(OH)_2$ saturated solution (pH 13.2). Chloride ions were added as NaCl in concentrations of 1, 5 and 10 wt./vol.%. The steel rod samples (prepared similarly to those used in the mortar tests) were immersed in the solutions so prepared and allowed to reach a stationary open circuit potential for 1 h. Afterwards, potentiodynamic polarization curves were obtained in a similar way as in mortar specimens. The experiments were repeated at least 3 times using a new specimen and fresh solution each time. Ohmic drop correction was performed in the same way as in mortar specimens.

From the anodic branch of the polarization curves, polarization resistance was evaluated as ΔE/ΔI between the corrosion potential (E_{corr}) and E_{corr} + 10 mV.

3. Results and discussion

Fig. 2 shows the polarization curves of steel in mortar immediately after the moist curing time and in SPS. Some differences are found. The corrosion potential is approximately 100 mV more positive in mortar than in SPS. Though in both sets of curves a passive zone ranging almost 800 mV is observed, the passive current densities are always higher in SPS than in mortar. Moreover, while in SPS the current density is almost constant and its value is close to 10^{-6} A/cm^2, in mortar specimens the current density increases slightly with the potential varying

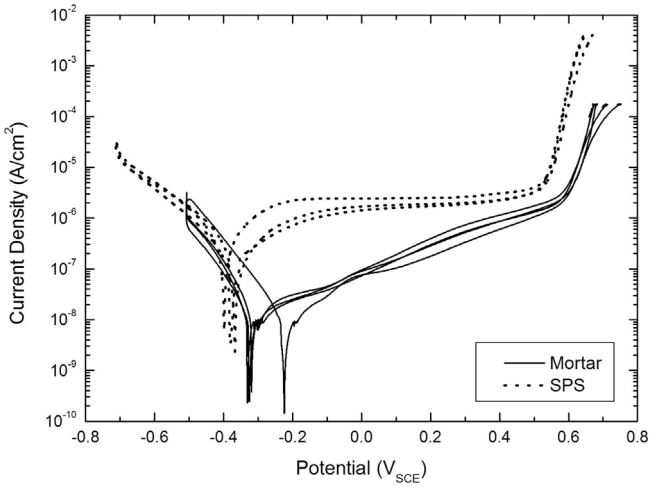

Fig. 2. Polarization curves of steel rods in mortar specimens and in simulated pore solution (SPS).

from 10^{-8} to 10^{-6} A/cm^2. At a potential equal to 0.5 V_{SCE} in SPS and 0.6 V_{SCE} in mortar, the current density increases abruptly until the total circulated current is of the order of 1 mA. At this point, the scan was reversed and no hysteresis was observed. This increase in current is associated to the oxygen evolution due to the decomposition of the solution; being the difference between the oxygen evolution potential in SPS and mortar ascribed to the difference in pH of both media (although some authors attribute this increase, referred to as transpassive dissolution, as a result from dielectric breakdown of the passive film [22]). Taking into account the suggestions made by Poursaee and Hansson [6] regarding the fact that for steel in pore solution the corrosion rate took about 3 days to drop to passive levels; some additional polarization curves were performed in SPS after immersing the steel specimens in SPS for 28 days to allow a pre-passivation (simulating the moist curing in mortar). The results showed that, while for pre-passivated specimens the corrosion potential increased some mV and the average passive current density decreased from 2×10^{-6} to 10^{-6} A/cm^2, the difference is not significant. For this reason, all tests in SPS in the present work were performed without a pre-passivation period, as in the usual way.

Fig. 3 shows the polarization curves of specimens embedded in mortar with different chloride contents. The curves were drawn immediately after the 28 days moist curing time (0 aging time). Repetitive results were obtained ($n = 4$) and representative curves are shown in Fig. 3 for the sake of simplicity. For low chloride contents (0, 0.5 and 2% Cl^-/cement), similar curves were obtained: from the corrosion potential an increase in current density with potential is observed, being the currents in the range 10^{-8} to 10^{-6} A/cm^2. At approximately 0.6 V_{SCE} the current density increases and no hysteresis is observed during the reverse scan, confirming that the increase in current density is due to the oxygen evolution. When increasing the chloride content of the mix (5 and 10% Cl^-/cement), a different behaviour is obtained. In both cases the corrosion potential is 400 mV lower than in the cases with low chloride contents. A passive zone is clearly identified with higher current densities than in the cases of low chloride contents but, unlike in the previous cases, the current density remains almost constant or increases with a small slope. In the case of 5% Cl^-/cement, the current density varies from 3×10^{-7} to 10^{-6} A/cm^2, and at 0.4 V_{SCE} the current density increases abruptly. When reversing the scan a high hysteresis loop is observed, indicating the existence of localized corrosion (pitting). In the case of 10% Cl^-/cement the passive current density is almost constant in the order of 2×10^{-7} A/cm^2. The initiation of pitting is also observed but at a potential considerably more negative than in the previous case (-0.15 V_{SCE}). Similar polarization curves were obtained when the specimens were kept at 98% RH for periods of 90 and 180 days after the moist curing.

At this stage it is worth mentioning that the chloride contents necessary to exhibit pitting in the present work are higher than most values reported in literature [23,24]. It is well known that when measuring pitting potentials (Epit) by potentiokinetic or quasi-stationary methods, one obtains values that depend on the scan rate used [25]. The fact that chloride contents necessary to exhibit pitting in the present work are higher (5% Cl/cem) than most values reported in literature could be explained if one considers that the scan rate used in the present work (0.2 mV/s) is higher than that suggested in the Standard ASTM G5 (0.167 mV/s) [26]. However, the difference is not so high and it seems improbable that the high chloride contents necessary to induce pitting could be accounted for the slight difference in scan rates. Besides, some authors [25] show that E_{pit} is more positive at a high scan rate than at a low scan rate but, in some cases, opposite results are noted: nobler Epit values are found at a lower scan rate. This can be explained taking into account that at a low scan rate it is possible the development and improvement of the protective properties of a passive film within the passivation potential range, which increases the resistance of metals to pitting. In particular, no systematic studies were found concerning the specific effect of the scan rate on E_{pit} for steel embedded in mortar or immersed in alkaline aqueous solutions containing chloride, so it was impossible to confirm if this fact (the apparently high scan rate used) is responsible for the above mentioned effect. Some papers deal with the effect of scan rate on the shape of the polarization curve; for instance, Mansfeld and Kendig [27] presented a general model concerning the choice of the scan rate for polarization measurement, while Poursaee and Hansson [28] showed results of polarization curves for steel in concrete at different scan rates. These works should be taken into account carefully for the selection of scan rates in potentiodynamic experiments and serve as a warning that uncritical use of potentiodynamic techniques can lead to erroneous results [27]. Another possibility (to explain the high chloride contents necessary to exhibit pitting) is to consider the surface finishing of the steel samples used. It is known the effect of surface finishing (roughness and/or the presence of a mill scale) on pitting potentials [25]. For mechanically prepared specimens the pitting potential decreases monotonously with the increasing surface roughness. When reading the literature concerning the critical chloride content in reinforced concrete chloride to induce pitting [23,24] it was observed that most of the data obtained in laboratory were taken from ribbed bars of steel with a mill scale bar steel not machined, while in the present work *as-received* AISI 1040 carbon steel smooth rods were used. Then, it is expected that this material shows a nobler behaviour than the ribbed bars, so higher E_{pit} are expected (or more aggressive conditions are probable necessary to observe the chloride attack).

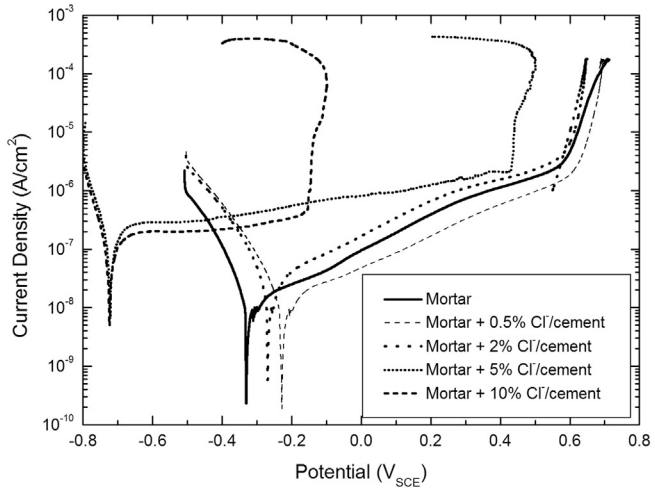

Fig. 3. Polarization curves of steel rods in mortar specimens with different chloride contents.

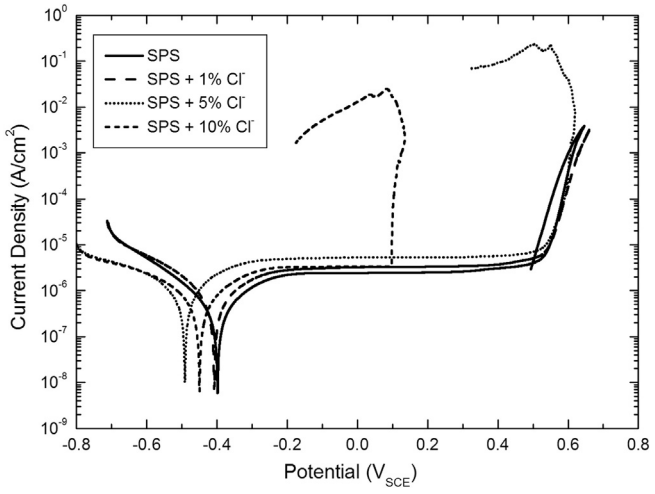

Fig. 4. Polarization curves of steel rods in simulated pore solution (SPS) with different chloride contents.

Fig. 4 shows the polarization curves of specimens immersed in SPS with different chloride contents. Repetitive results were obtained ($n = 3$ at least) and representative curves are shown in Fig. 4 for the sake of simplicity. For low chloride contents (0 and 1 wt./vol.%), similar curves were obtained: from the corrosion potential a passive zone ranging >800 mV is observed, the passive current density is almost constant and its value is close to 2×10^{-6} A/cm^2. At approximately 0.5 V_{SCE} the current density increases and no hysteresis is observed during the reverse scan, confirming that the increase in current density is due to the oxygen evolution. When increasing the chloride content of the solution (5 and 10 wt./vol.%), a different behaviour is obtained. In both cases the corrosion potential is 50–100 mV lower than in the cases with low chloride contents. A passive zone is clearly identified in both cases, being the current density higher in the most chloride concentrated solution. Unlike in the previous cases, the existence of localized attack was observed because of the abrupt increase of the current density and the presence of a hysteresis loop when the scan was reversed. In the solution with 5 wt./vol.% of chloride, the potential at which the localized attack begins (E_{pit}) coincides with the oxygen evolution potential (0.5 V_{SCE}). In the solution with 10 wt./vol.% of chloride, the E_{pit} is considerably lower (0.1 V_{SCE}).

Table 2 shows the average values and standard deviation of the corrosion potential (E_{corr}) obtained in mortar (at different aging times) and in SPS, with different chloride contents.

In order to facilitate the comparison, Fig. 5 shows only the average value of the E_{corr}. In the case of mortar tests, the E_{corr} is almost constant for chloride contents between 0 and 2%. For higher chloride contents a significantly decrease in the E_{corr} is observed, and then the E_{corr} remains constant up to 10% of chloride content. No significant effect of the aging time was observed. On the other hand, the addition of chloride to SPS induces a slight and constant decrease in the E_{corr} with additions of chloride up to 5%, and then it remains almost constant. From this figure it seems that the E_{corr} measured in mortar is equal to that measured in SPS when the chloride content is around 3%.

To characterize the passive state of the steel in mortar at different aging times and in SPS, with different chloride contents, the passive current density (current density at a potential 300 mV higher than the E_{corr}) was measured. Table 3 shows the average and standard deviation of the passive current density (I_{pass}) so obtained. It should be noted that, in some cases, the deviation in the I_{pass} is appreciable. For the sake of simplicity Fig. 6 shows only the average values of I_{pass}. As expected, in general terms, the higher the chloride content the higher the I_{pass}. In the case of mortar specimens no matter the aging time, the I_{pass} shows an increase when increasing the chloride content between 0 and 5%. For higher chloride concentrations, the behaviour observed depends on the aging time: while for 0 days aging time the I_{pass} remains constant for chloride contents between 5 and 10%, for higher aging times an increase in the I_{pass} was observed. The higher the aging time the higher the increase in I_{pass}. In the case of tests performed in SPS, the I_{pass} increases monotonously with the chloride content. Besides, in SPS the I_{pass} is at least one order of magnitude higher than in mortar, independently of the chloride content.

As observed in the polarization curves, pitting was found only for chloride contents higher than 5%, both in mortar and in SPS. Fig. 7 shows the average and standard deviation of the E_{pit} measured on mortar specimens with different aging times and in SPS. The first observation is that the aging time has little or no effect on the E_{pit} of steel embedded in mortar. For 5% chloride concentration the E_{pit} was close to 0.5 V_{SCE} while for 10% chloride concentration E_{pit} is close to −0.2 V_{SCE}. In the case of tests on SPS, the average E_{pit} for 5% of chloride is 0.54 V_{SCE} and decreases to 0.08 V_{SCE} when the chloride content is 10%. It can be observed that, under certain conditions, the deviation in the E_{pit} is appreciable. This fact has been previously reported by Li and Sagüés [5] who mentioned that results from a large series of repeat tests show significant deviation. Similar E_{pit} were measured in mortar with 5% Cl^-/cement and in SPS with 5 wt./vol.% of chloride.

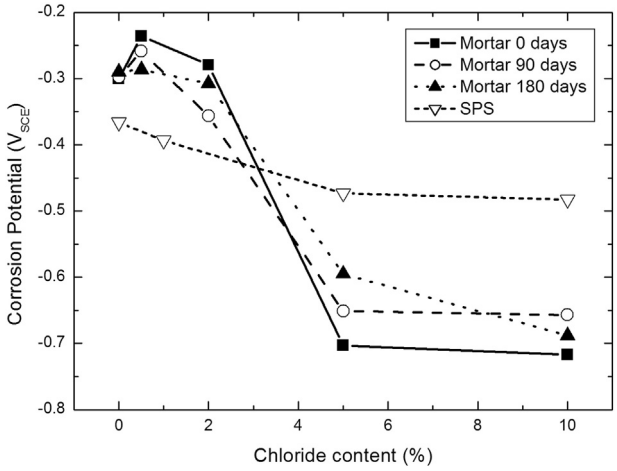

Fig. 5. Corrosion potential of steel rods in mortar specimens after different aging times and in simulated pore solution (SPS), as a function of the chloride content.

Table 4 shows the average values and standard deviation of the polarization resistance (R_P) obtained in mortar (at different aging times) and in SPS, with different chloride contents. Again, this parameter shows an appreciable deviation under certain conditions.

In order to facilitate the comparison, Fig. 8 shows only the average value of the R_P. The first observation that arises from the figure is that the aging time has little or no effect on the R_P in mortar tests. However, the chloride content has a significant effect on the R_P: when the chloride content increases from 0 to 10%, the R_P decreases one order of magnitude, and hence the corrosion rate that is inversely proportional to this value [29] increases one order of magnitude. A similar tendency is observed in SPS but the R_P in this case is one order of magnitude lower than in mortar, for all the range of chloride contents studied, revealing the fact that the SPS is more aggressive to the steel than mortar.

As it was mentioned in the Introduction section one of the objectives of the present work was to determine whether the SPS simulates the electrochemical behaviour shown by the steel embedded in cementitiuos materials. As it can be observed in Fig. 2 the polarization curves in mortar and in SPS, though quite similar in shape, differ in the values of the different electrochemical parameters. From Tables 2, 3 and 4 it can be observed that the E_{corr} is 60 mV lower, the I_{pass} is 25 times higher and the R_P is 14 times lower in SPS than in mortar. All these electrochemical parameters reflect the fact that the SPS is more aggressive to the steel than the mortar itself. This aggressiveness cannot be attributed neither to the pH of the SPS, that is close to 13.2 and quite

Table 2
Corrosion potential (in V_{SCE}) of steel rods embedded in mortar with different aging times and immersed in simulated pore solution (SPS), with different chloride contents. In mortar, chloride contents are expressed as wt.% Cl^-/cement, while in SPS are expressed as % Cl^- wt./vol.

	0% Cl^-	0.5% Cl^-	1% Cl^-	2% Cl^-	5% Cl^-	10% Cl^-
Mortar 0 days	−0.300 ± 0.052	−0.236 ± 0.035	–	−0.279 ± 0.013	−0.703 ± 0.028	−0.717 ± 0.016
Mortar 90 days	−0.297 ± 0.006	−0.259 ± 0.012	–	−0.357 ± 0.047	−0.651 ± 0.076	−0.657 ± 0.049
Mortar 180 days	−0.290 ± 0.003	−0.286 ± 0.006	–	−0.308 ± 0.008	−0.595 ± 0.113	−0.688 ± 0.021
SPS	−0.366 ± 0.033	–	−0.393 ± 0.021	–	−0.473 ± 0.065	−0.483 ± 0.042

Table 3
Passive current density (in μA/cm^2) of steel rods embedded in mortar with different aging times, and immersed in simulated pore solution (SPS) with different chloride contents, at a potential 0.3 V higher than the corrosion potential. In mortar, chloride contents are expressed as %wt. Cl^-/cement, while in SPS are expressed as %Cl^- wt./vol.

	0% Cl^-	0.5% Cl^-	1% Cl^-	2% Cl^-	5% Cl^-	10% Cl^-
Mortar 0 days	0.077 ± 0.014	0.100 ± 0.033	–	0.17 ± 0.05	0.300 ± 0.025	0.260 ± 0.098
Mortar 90 days	0.043 ± 0.006	0.047 ± 0.007	–	0.078 ± 0.045	0.460 ± 0.057	0.860 ± 0.760
Mortar 180 days	0.065 ± 0.005	0.071 ± 0.016	–	0.110 ± 0.036	0.390 ± 0.230	2.2 ± 2.3
SPS	1.9 ± 1.1	–	2.0 ± 0.6	–	6.1 ± 2.8	8.1 ± 7.7

similar to that of not carbonated mortar, nor to the pre-passivation period (as it was shown above). Then, the main conclusion is that the SPS is not fully representative of the behaviour of the steel in mortar. However, the results obtained by using this solution to evaluate the corrosion resistance of steel in concrete are conservative and thus useful, but results must be considered with caution.

The other issue that the present work is aimed at is to determine the chloride content in SPS that yields a similar behaviour in a cementitious material contaminated with chloride. To this purpose different electrochemical parameters can be taken as reference. If the E_{corr} is considered it has been shown in Fig. 5 that the E_{corr} measured in mortar equals that measured in SPS when the chloride content is around 3%. Besides, other data are comparable: E_{corr} for SPS with no chloride is comparable to that of mortar with 2% Cl^-/cement; SPS with 5 and 10% wt./vol.% are comparable to mortar containing 4 wt./cement chloride. However, if the I_{pass} is considered, from Fig. 6, it can be concluded that I_{pass} measured in mortar with 10% Cl^-/cement (at 180 days aging time) is approximately equal to that measured in SPS with 0 and 1 wt./vol.% of chloride. When the E_{pit} is considered, Fig. 7 shows that steel in mortar with 5% Cl^-/cement behaves as in SPS with 5 wt./vol.% of chloride.

Finally, taking into account the R_P, from Fig. 8, it can be inferred that the R_P value obtained in SPS with 1 wt./vol.% of chloride is approximately equal to that obtained in mortar with additions of chloride higher than 5% Cl^-/cement. All these data has been included in Fig. 9, together with some data obtained from literature [8,30]. In [8] it is stated that a mortar with 0.4% Cl^-/cement behaves close to a SPS with 1.5 wt./vol.% of chloride, and a mortar with 3% Cl^-/cement behaves close to a SPS with 8 wt./vol.% of chloride. Anders et al. [30] analysed the chloride content of pore solution extracted from cylinders of cement paste with known admixed sodium chloride content assuming that these data are applicable to corrosion testing of rebars in synthetic concrete pore solution. Fig. 9 shows the results of Anders et al. [30] converted to the experimental conditions of the present work (w/c = 0.6) by employing the technique proposed by the authors (assuming 50% hydration). It can be observed that the results obtained in the present work differ from those of the literature [8,30], no matter the parameter considered. It is clear from Fig. 9 that the relationship between the chloride content in mortar and in SPS that yields similar steel corrosion behaviour depends on the electrochemical parameter chosen as reference. To sum up, a direct comparison is not straightforward. Therefore, the use of SPS, with or without chloride, is adequate when comparing different materials, surface treatments, the effect of inhibitors, etc. but, by no means, the results obtained reflect the behaviour of those materials in concrete (corrosion rate, chloride threshold for corrosion initiation, etc.).

4. Conclusions

- The polarization curves of steel in mortar and in SPS, though quite similar in shape, differ in the values of the different electrochemical parameters.
- The use of pre-passivated specimens in SPS (simulating the 28 days moist curing time in mortar) do not modify the results.
- The SPS is not fully representative of the behaviour of steel in mortar, being more aggressive, so that it provides conservative results.
- The relationship between the chloride content in mortar and in SPS that yields similar behaviour could not be established because it depends on the electrochemical parameter considered.
- The use of SPS with different chloride levels is useful when comparing the corrosion behaviour of different materials, but an extrapolation to the behaviour in mortar is not adequate.

Acknowledgements

The financial support of the CONICET (Consejo Nacional de Investigaciones Científicas y Técnicas) (PIP 2011/00010), the Universidad Nacional de San Martín (UNSAM) (PROG07A/1) and of the FONCYT (PICT 2013/0239), Secretaría para la Tecnología, la Ciencia y la Innovación Productiva, Argentina, is acknowledged.

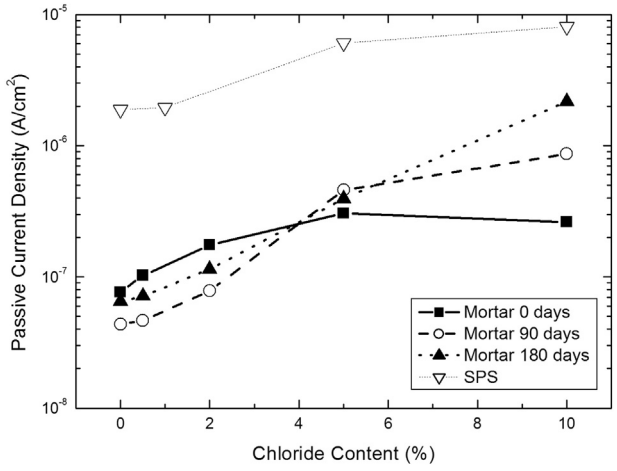

Fig. 6. Passive current density of steel rods in mortar specimens after different aging times and in simulated pore solution (SPS), as a function of the chloride content.

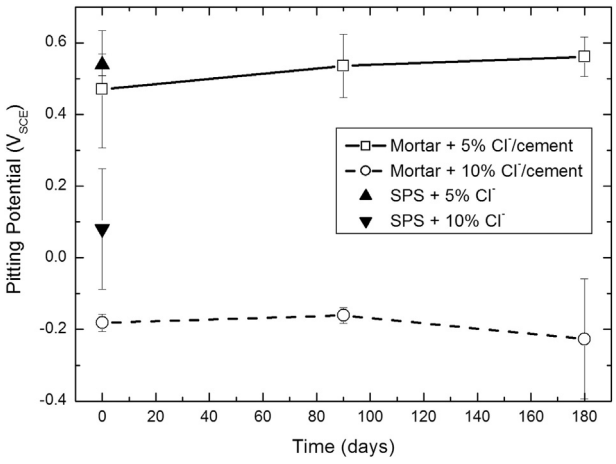

Fig. 7. Pitting potential of steel rods in mortar specimens and in simulated pore solution (SPS) with different chloride contents, as a function of the aging time.

Table 4
Polarization resistance (in kohm · cm^2) of steel rods embedded in mortar with different aging times, and immersed in simulated pore solution (SPS) with different chloride contents. In mortar, chloride contents are expressed as wt.% Cl^-/cement, while in SPS are expressed as %Cl^- wt./vol.

	0% Cl^-	0.5% Cl^-	1% Cl^-	2% Cl^-	5% Cl^-	10% Cl^-
Mortar 0 days	2230 ± 541	1800 ± 475	–	1220 ± 264	243 ± 189	268 ± 187
Mortar 90 days	3270 ± 522	2640 ± 84	–	1610 ± 620	397 ± 270	205 ± 45
Mortar 180 days	1750 ± 255	1470 ± 665	–	1360 ± 403	626 ± 122	293 ± 264
SPS	155 ± 67	–	186 ± 181	–	49 ± 19	39 ± 18

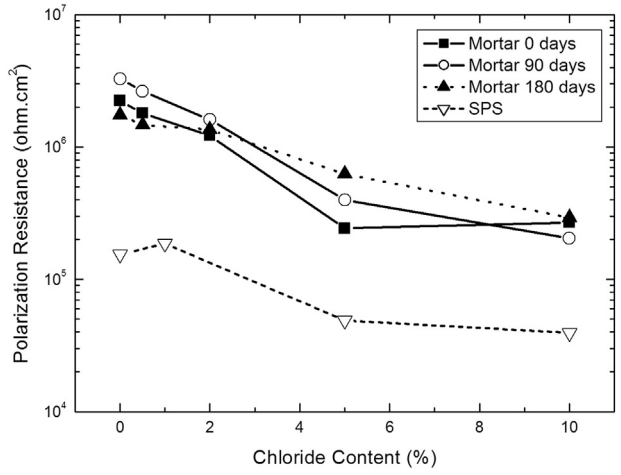

Fig. 8. Polarization resistance of steel rods in mortar specimens after different aging times and in simulated pore solution (SPS), as a function of the chloride content.

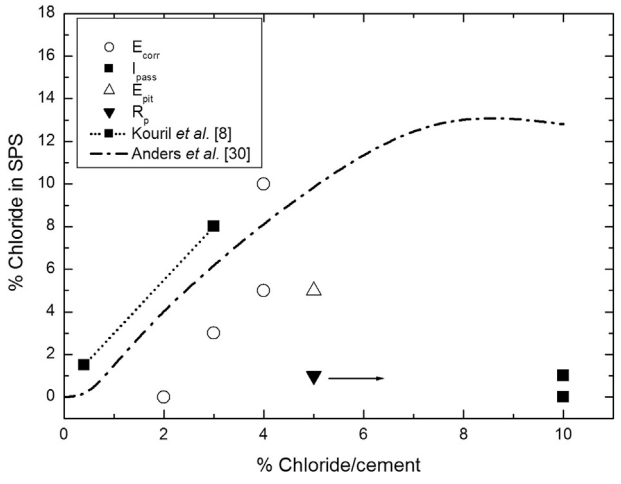

Fig. 9. Equivalence between chloride content in simulated pore solution (SPS) and in mortar (as % chloride/cement), based on different electrochemical parameters (E_{corr}: corrosion potential; I_{pass}: passive current density; E_{pit}: pitting potential; R_p: polarization resistance) measured in the present work. Data obtained from literature [8,30] are also shown.

References

[1] S. Goñi, C. Andrade, Synthetic concrete pore solution chemistry and rebar corrosion rate in the presence of chlorides, Cem. Concr. Res. 20 (1990) 525–539.
[2] L.T. Mammoliti, L.C. Brown, C.M. Hansson, B.B. Hope, The influence of surface finish of reinforcing steel and pH of the test solution on the chloride threshold concentration for corrosion initiation in synthetic pore solutions, Cem. Concr. Res. 26 (1996) 545–550.
[3] C.J. Kitowski, H.G. Wheat, Effect of chlorides on reinforcing steel exposed to simulated concrete solutions, Corrosion 53 (1997) 216–226.
[4] C. Alonso, M. Castellote, C. Andrade, Chloride threshold dependence of pitting potential of reinforcements, Electrochim. Acta 47 (2002) 3469–3481.
[5] L. Li, A.A. Sagüés, Chloride corrosion threshold of reinforcing steel in alkaline solutions – cyclic polarization behavior, Corrosion 58 (2002) 305–316.
[6] A. Poursaee, C.M. Hansson, Reinforcing steel passivation in mortar and pore solution, Cem. Concr. Res. 37 (2007) 1127–1133.
[7] P. Ghods, O.B. Isgor, G. McRae, T. Miller, The effect of concrete pore solution composition on the quality of passive oxide films on black steel reinforcement, Cem. Concr. Compos. 31 (2009) 2–11.
[8] M. Kouřil, P. Novák, M. Bojko, Threshold chloride concentration for stainless steels activation in concrete pore solutions, Cem. Concr. Res. 40 (2010) 431–436.
[9] L. Yang, K. Chiang, H. Yu, R.T. Pabalan, B. Dasgupta, L. Ibarra, Threshold chloride levels for localized carbon steel corrosion in simulated concrete pore solutions using coupled multielectrode array sensors, Corrosion 70 (2014) 850–857.
[10] A. Macías, C. Andrade, Corrosion rate of galvanized steel immersed in saturated solutions of $Ca(OH)_2$ in the pH range 12–13.8, Br. Corros. J. 18 (1983) 82–87.
[11] B. Lin, Y. Xu, Corrosion behavior of hot-dip galvanized reinforcing steel using electrochemical impedance spectroscopy, Adv. Mater. Res. 250-253 (2011) 22–227.
[12] P. Ling, Y. Wang, Effect of chloride on corrosion behavior of reinforcing steel HRB335, Adv. Mater. Res. 391-392 (2012) 1342–1345.
[13] H. Yu, K.-T.K. Chiang, L. Yang, Threshold chloride level and characteristics of reinforcement corrosion initiation in simulated concrete pore solutions, Constr. Build. Mater. 26 (2012) 723–729.
[14] H.E. Jamil, M.F. Mortemor, R. Boulif, A. Shriri, M.G.S. Ferreira, An electrochemical and analytical approach to the inhibition mechanism of an amino-alcohol-based corrosion inhibitor for reinforced concrete, Electrochim. Acta 48 (2003) 3509–3518.
[15] S.M. Abd El Haleem, S. Abd El Wanees, E.E. Abd El Aal, A. Diab, Environmental factors affecting the corrosion behavior of reinforcing steel II. Role of some anions in the initiation and inhibition of pitting corrosion of steel in $Ca(OH)_2$ solutions, Corros. Sci. 52 (2010) 292–302.
[16] X.-P. Wang, R.-G. Du, Y.-F. Zhu, Y. Guo, W. Chen, Z. Yang, S. Dong, C. Lin, Sodium nitrite-based corrosion inhibitor for reinforcing steel in simulated polluted concrete pore solutions, ECS Trans. 50 (2012) 43–51.
[17] N.A. Almobarak, M.M. El-Nagger, R.S. Al-Mufraj, O.A. Al-Zoghbi, Carboxylic acids: pitting corrosion inhibitors for carbon steel in alkaline medium and in the presence of chloride, Chem. Technol. Fuels Oils 50 (2014) 170–178.
[18] C.Y. Rha, W.S. Kim, J.W. Kim, H.H. Park, Relationship between microstructure and electrochemical characteristics in steel corrosion, Appl. Surf. Sci. 169-170 (2001) 587–592.
[19] J.A. González, J.M. Miranda, E. Otero, S. Feliú, Effect of electrochemically reactive rust layers on the corrosion of steel in a $Ca(OH)_2$ solution, Corros. Sci. 49 (2007) 436–448.
[20] G.A. El-Mahdy, M.M. Hegazy, M.M. Eissa, A.M. Fathy, F.M. Sayed, N. El-Manakhly, Hamad-Al-Lohedan, Influence of heat and laser treatments on the corrodibility of the reinforced carbon steel, Int. J. Electrochem. Sci. 7 (2012) 6677–6692.
[21] A.N. Al-Negheimish, A. Alhozaimy, R.R. Hussain, R. Al-Zaid, J.K. Singh, D.D.N. Singh, Role of manganese sulfide inclusions in steel rebar in the formation and breakdown of passive films in concrete pore solutions, Corrosion 70 (2014) 74–86.
[22] ACI Committee 222, Protection of Metals in Concrete Against Corrosion, ACI 222R-01, ACI Manual of Concrete Practice, Michigan 2004, p. 5.
[23] C. Alonso, C. Andrade, M. Castellote, P. Castro, Chloride threshold values to depassivate reinforcing bars embedded in a standardized OPC mortar, Cem. Concr. Res. 30 (2000) 1047–1055.
[24] U. Angst, B. Elsener, C. Larsen, Ø. Vennesland, Critical chloride content in reinforced concrete-a review, Cem. Concr. Res. 39 (2009) 1122–1138.
[25] Z. Szklarska-Smialowska, Pitting and Crevice Corrosion, NACE International, Houston, 2005.
[26] ASTM Standard G0005-94R04 Reference Test Method for Making Potentiostatic and Potentiodynamic Anodic Polarization Measurements, 1999 Annual Book of ASTM Standard, Vol. 04.02, ASTM, West Conshohokem, PA, 1999.
[27] F. Mansfeld, M. Kendig, Concerning the choice of scan rate in polarization measurements, Corrosion 37 (1981) 545–546.
[28] A. Poursaee, C.M. Hansson, Potential pitfalls in assessing chloride-induced corrosion of steel in concrete, Cem. Concr. Res. 39 (2009) 391–400.
[29] C. Andrade, C. Alonso, Corrosion rate monitoring in the laboratory and on-site, Constr. Build. Mater. 10 (1996) 315–328.
[30] K. Anders, B. Bergsma, C. Hansson, Chloride concentration in the pore solution of Portland cement paste and Portland cement concrete, Cem. Concr. Res. 63 (2014) 35–37.